

1 **Pressure drop modelling in sand filters in micro-irrigation using**
2 **gradient boosted regression trees**

3 P.J. García Nieto^{a,*}, E. García–Gonzalo^a, G. Arbat^b, M. Duran–Ros^b, F. Ramírez de
4 Cartagena^b, J. Puig-Bargués^b

5 ^aDepartment of Mathematics, Faculty of Sciences, University of Oviedo, 33007 Oviedo, Spain

6 ^bDepartment of Chemical and Agricultural Engineering and Technology, University of Girona, 17071
7 Girona, Catalonia, Spain

8

9 **Abstract**

10 Filters are essential for guaranteeing the good performance of microirrigation systems.
11 Pressure losses across filters should be known for the proper design and management of
12 this irrigation equipment. Pressure losses produced by filtering media in sand filters can
13 be computed using Ergun or Kozeny-Karman equations, which require knowledge,
14 among other parameters, of the sphericity of the filter medium. As this parameter is not
15 easy to determine, it is useful to explore the performance of alternative computing
16 methods that can avoid requiring knowledge of sphericity. In this paper, taking as starting
17 point the nonparametric machine learning approach known as the gradient boosted
18 regression tree (GBRT) approach and hybridising it with the differential evolution (DE)
19 technique, the pressure drop in sand filters used in microirrigation has been modelled. For
20 different filtering materials such as modified glass, crushed glass, silica sand and glass
21 microspheres, experimental data of pressure drop for velocities between 0.004 and 0.025
22 m s⁻¹ was collected and the model built. The results demonstrated that DE–GBRT–based
23 model was able to accurately predict pressure drop. The model also allowed ranking of

*Corresponding author. Tel.: +34-985103417; fax: +34-985103354.
E-mail address: lato@orion.ciencias.uniovi.es (P.J. García Nieto).

24 the importance of the independent variables examined within the model. Taking into
25 account this ranking, and using only the main variables, a simplified method with an
26 improved coefficient of determination was constructed.

27

28 *Keywords:* Regression trees; Gradient boosting; Differential evolution; Drip irrigation;
29 Sand filters

30

31 **Nomenclature**

32

ABC	Artificial bee colony
b_{jm}	Constant value calculated for the region R_{jm}
C_o	Cover of the GBRT algorithm
$CART$	Classification and Regression Trees
D_{eq}	Equivalent diameter, m
DE	Differential evolution
F_m	Weak model that predicts the mean y of the training set
F_q	Frequency of the GBRT algorithm
$F_0(x)$	Constant function
$\hat{F}(x)$	an estimate of the function $F^*(x)$
G_a	Gain of the GBRT algorithm
GA	Genetic algorithm
$GBRT$	Gradient boosted regression tree
GR	Parameter that controls the recombination rate

H	Set of arbitrary differentiable functions
h	Weak learner function
$h_i(x)$	Weighted sum of functions
$h_m(x)$	Decision tree
J_m	Number of terminal nodes in the tree model
NP	Noisy random vectors
$L()$	Loss function
m	Weighted medium mass, kg
m_{og}	Overall mass of the grains, kg
<i>MARS</i>	multivariate adaptive regression splines
<i>MCW</i>	Minimum child weight of GBRT algorithm
<i>MDS</i>	Minimum delta step of GBRT algorithm
n	Number of observed data
N	Number of grains
<i>Nrounds</i>	Maximum number of iterations of the GBRT algorithm
p	Index of the individual in the population
<i>PSO</i>	Particle swarm optimization
r_{im}	Pseudo-residuals
RMSE	Root mean square error
R^2	Coefficient of determination
<i>SR</i>	Subsample ratio of the GBRT algorithm
SS_{tot}	Total sum of squares
SS_{reg}	Regression sum of squares
SS_{err}	Residual sum of squares

\mathbf{t}_m^g	Trial vectors
V_m	Medium volume, m ³
V_w	Volume of the additional water, m ³
V_f	Final volume of the water and medium mixture, m ³
V	Mean flow velocity, m s ⁻¹
\mathbf{x}_p^g	Original vectors
$(\Delta p / \Delta L)$	Pressure drop per unit length
Δ	Step value over each tree's weight estimation
ε	Medium porosity
η	Learning rate of GBRT algorithm
ρ_b	Bulk density of each medium, kg m ⁻³
ρ_r	Real density of each medium, kg m ⁻³
ϕ	Sphericity factor
γ	Minimum loss reduction of the GBRT algorithm
Ω	Penalty function that controls the model complexity

33

34 **1. Introduction**

35 Proper irrigation water filtration is essential to ensure the successful continuous long-term
36 operation of microirrigation systems (Clark, Haman, Prochaska, & Yitayew, 2007). By
37 following good maintenance practices, which includes filtration, the longevity of some
38 subsurface microirrigation systems have reached 26.5 years (Lamm & Rogers, 2017).
39 Screen, disc, media and hydro-cyclone filters are common filter types that are used in
40 microirrigation systems. The choice of filter type will basically depend on the quality of

41 water source, the flow rate of the irrigation system and the desired filtered water quality
42 for avoiding emitter clogging (Clark et al, 2007).

43

44 Irrigation engineers require knowledge of the pressure drop across the filter to properly
45 design and manage this important system component which is related to water and energy
46 consumption as well as pollutant removal efficiency (Duran-Ros, Puig-Bargués, Arbat,
47 Barragán, & Ramírez de Cartagena, 2009). Mathematical models have been developed
48 using dimensional analysis for describing pressure drops across screens (Wu, Chen, Liu,
49 Yin, & Niu, 2014b; Zong, Zheng, Liu & Li, 2015), disc (Yurdem, Demir, &
50 Degirmencioglu, 2008; Wu et al., 2014a), hydrocyclone (Yurdem, Demir, &
51 Degirmencioglu, 2008) and in sand media filters (Elbana, Ramírez de Cartagena, & Puig-
52 Bargués, 2013). These models did not consider the specific effect of the different filter
53 components (filtration zone and auxiliary elements) on pressure loss. In sand media
54 filters, pressure loss clearly vary across the filter media, the underdrain and diffuser
55 platter, and the backflushing valve (Bové et al., 2015b; Burt, 2010; Mesquita, Testezlaf
56 & Ramirez, 2012).

57

58 Bové et al. (2015a) experimentally analysed the pressure drop across different sand and
59 recycled glass media in a microirrigation sand filter. Although the Ergun equation showed
60 the best prediction accuracy for predicting the pressure drop, multi linear regression
61 equations had better performance than the Kozeny–Carman equation, which is a
62 simplification of the Ergun equation. However, these equations require parameters
63 defining the filter media such as equivalent diameter and sphericity which are difficult to
64 obtain.

65 García-Nieto et al. (2017) used a hybrid model artificial bee colony (ABC)-multivariate
66 adaptive regression splines (MARS) which satisfactorily computed pressure loss across
67 filtration beds without the need for sphericity. This work suggests that other alternative
68 methods, specifically a hybrid methodology that combines the gradient boosted
69 regression tree (GBRT) approach with the differential evolution (DE) optimisation
70 algorithm (Storn, & Price, 1997; Price, Storn, & Lampinen, 2005; Feoktistov, 2006;
71 Rocca, Oliveri, & Massa, 2011), could also be used to predict pressure drops in the
72 granular filters used in microirrigation systems.

73

74 GBRT models are supervised machine learning procedures that can be used for
75 multivariate classification and regression (Vapnik, 1998; Friedman, 2002; Schapire,
76 2003; Bühlman & Hothorn, 2007; Hastie et al., 2003). GBRT models build competitive,
77 highly robust procedures that are particularly appropriate for treating not very clean data
78 (Hastie et al., 2003). They are very flexible models that can be easily be customised for
79 any data-driven task. They are straightforward to implement and have been very
80 successful in data-mining and machine-learning challenges (Natekin & Knoll, 2013). One
81 of the reasons for their success could be that tree boosting takes the bias-variance trade-
82 off into consideration while fitting the models (Nielsen, 2016). For example, GBRT
83 models have been effective in predicting biological parameters in environmental
84 problems such as forecasting wind variables (Landry et al., 2016), solar power generation
85 prediction (Persson et al., 2017) and short-term waste estimation (Johnson et al., 2017).

86

87 Differential evolution (DE) is a metaheuristic evolutionary global method, derived from
88 genetic algorithm (GA), intrinsically capable of solving multidimensional optimisation

89 problems involving continuous variables. As with other evolutionary computation
90 algorithms such as particle swarm optimisation (PSO) (Eberhart et al., 2001; Clerc, 2006;
91 Olsson, 2011) or ant colony optimisation (Dorigo & Stützle, 2004), DE is a bio-inspired
92 algorithm that generates high-quality solutions to optimisation problems by means of bio-
93 inspired operators such as mutation, recombination and selection (Storn & Price, 1997;
94 Price, Storn & Lampinen, 2005; Simon, 2013; Yang et al., 2013).

95

96 The main objective of the present study was to develop a hybrid algorithm using DE
97 optimising GBRT parameters (DE–GBRT) to predict the pressure drop per unit length
98 ($\Delta p / \Delta L$) across sand and recycled glass media from the physical input parameters of the
99 filtration media used in media filters.

100

101 **2. Materials and methods**

102 *2.1. Experimental setup*

103 The experimental setup providing the considered data set is described in Bové et al.
104 (2015a). In a laboratory filter, which was a scaled version of a commercial microirrigation
105 media filter (Arbat et al., 2013), pressure losses of four different filtration materials (silica
106 sand, crushed recycled glass, surface modified glass and microspheres) with grain sizes
107 between 0.63 and 1.50 mm were measured at surface velocities ranging from 0.004 to
108 0.025 m s⁻¹ under pressures ranging between 4,631 and 275,630 Pa.

109

110 *2.2. Variables involved in the model*

111 Data obtained from the experiment gave the pressure drop per unit length ($\Delta p / \Delta L$), as
112 the output variable. The input variables were the filter media type (as category), media
113 bulk and real density, porosity, equivalent diameter, sphericity or shape factor, flow
114 surface velocity and average grain size. Procedures for obtaining these variables are
115 described in Bové et al. (2015a).

116

117 *2.3. Computational procedure*

118 *2.3.1. Gradient boosting regression tree (GBRT)*

119 Gradient boosting is a machine learning method used for classification and regression that
120 constructs a model from a set of weak models or learners, that are, usually, decision trees.
121 It builds the model by stages, as is typical for boosting methods, and obtains a single
122 strong ensemble model optimising a differentiable loss function (Breinman et al. 1984;
123 Vapnik, 1998; Friedman et al., 2000; Friedman, 2001; Friedman, 2002; Schapire, 2003;
124 Bühlman & Hothorn 2007; Hastie et al., 2003).

125

126 It can be described as a least-squares regression method, where the aim is to teach a model
127 F to predict the values $\hat{y} = F(x)$, minimizing the mean squared error $(\hat{y} - y)^2$, being y
128 the true values from the training set. At each stage $1 \leq m \leq M$ of gradient boosting, we
129 have a weak model F_m that predicts the mean y of the training set. The gradient boosting
130 algorithm improves F_m constructing a new model F_{m+1} that adds an estimator h to improve
131 the previous model $F_{m+1}(x) = F_m(x) + h(x)$. To find h , the gradient boosting method

132 takes into account that, to have a perfect h (Friedman et al., 2000; Schapire, 2003;
 133 Bühlman & Hothorn, 2007; Hastie et al., 2003):

$$F_{m+1}(x) = F_m(x) + h(x) = y \quad (1)$$

134 that is,

135

$$h(x) = y - F_m(x) \quad (2)$$

136 Thus, gradient boosting will perform the fitting of h to the residual $y - F_m(x)$. In each
 137 stage, F_{m+1} is constructed as a correction of its predecessor F_m . We can generalise this
 138 explanation to other loss functions different from squared error, taking into account that
 139 residuals $y - F(x)$ are the negative gradients of the loss function $\frac{1}{2}(y - F(x))^2$.

140

141 As in other supervised learning problems, we have an output variable y and a set of input
 142 variables x . The objective is to find an estimate $\hat{F}(x)$ of the function $F^*(x)$ that
 143 minimises the value of some loss function $L(y, F(x))$ using a training set
 144 $\{(x_1, y_1), (x_2, y_2), \dots, (x_n, y_n)\}$ of already known values of x and their corresponding
 145 values of y , (Friedman, 2002; Schapire, 2003; Bühlman & Hothorn, 2007; Hastie et al.,
 146 2003; Mayr et al., 2014a,b; Taieb & Hyndman, 2014; Döpke et al., 2017):

$$\hat{F} = \arg \min_F E_{x,y} [L(y, F(x))] \quad (3)$$

The gradient boosting method approximates y with a weighted sum of functions $h_i(x)$
 from some class H , called weak learners:

$$F(x) = \sum_{i=1}^M \gamma_i h_i(x) + \text{const} \quad (4)$$

Using the empirical risk minimisation principle, the method looks for an approximation $\hat{F}(x)$ that minimises the average value of the loss function on the training set. It starts with a model, that consists in a constant function $F_0(x)$, and step by step expands its value in a greedy way (Hastie et al., 2003; Taieb & Hyndman, 2014; Döpke et al., 2017):

$$F_0(x) = \arg \min_{\gamma} \sum_{i=1}^n L(y_i, \gamma) \quad (5)$$

$$F_m(x) = F_{m-1}(x) + \arg \min_{h \in H} \sum_{i=1}^n L(y_i, F_{m-1}(x_i) + h(x_i)) \quad (6)$$

where $h \in H$ is a weak learner function.

As choosing the best function h at every stage for an arbitrary loss function L is a computationally infeasible optimization problem, a simplification is applied and a steepest descent method is used to solve this minimization problem. Given the continuous case, where H is the set of arbitrary differentiable functions, the model is updated following the equations (Hastie et al., 2003; Taieb & Hyndman 2014; Döpke et al., 2017):

$$F_m(x) = F_{m-1}(x) - \gamma_m \sum_{i=1}^n \nabla_{F_{m-1}} L(y_i, F_{m-1}(x_i)) \quad (7)$$

$$\gamma_m = \arg \min_{\gamma} \sum_{i=1}^n L \left(y_i, F_{m-1}(x_i) - \gamma \frac{\partial L(y_i, F_{m-1}(x_i))}{\partial F_{m-1}(x_i)} \right) \quad (8)$$

147 where the derivatives are obtained with respect to the functions F_i for $i \in \{1, 2, \dots, m\}$. If we
 148 are treating a discrete case, where the set H is finite, the candidate function h that is closest
 149 to the gradient of L will be chosen and the coefficient γ can then be calculated using line
 150 search in equations (7) and (8). This is a heuristic approach and will not give an exact
 151 solution to problem, but a good approximation.

152

153 The generic gradient boosting method can be described by a pseudocode (Friedman,
 154 2002; Hastie et al., 2003; Taieb & Hyndman, 2014; Döpke et al., 2017):

155 ➤ Input: differentiable loss function $L(y, F(x))$, training set $\{(x_i, y_i)\}_{i=1}^n$ and
 156 iteration number M .

157 ➤ Algorithm:

158 1. Initialize model using a constant value:

159
$$F_0(x) = \arg \min_{\gamma} \sum_{i=1}^n L(y_i, \gamma)$$

160 2. For $m = 1$ to M :

161 • Compute so-called *pseudo-residuals*:

162
$$r_{im} = - \left[\frac{\partial L(y_i, F(x_i))}{\partial F(x_i)} \right]_{F(x)=F_{m-1}(x)} \quad \text{for } i = 1, \dots, n$$

163 • Fit a weak learner $h_m(x)$ to the pseudo-residuals using the training set

164
$$\{(x_i, r_{im})\}_{i=1}^n.$$

165 • Calculate the multiplier γ_m solving the one-dimensional optimisation
 166 problem:

167
$$\gamma_m = \arg \min_{\gamma} \sum_{i=1}^n L(y_i, F_{m-1}(x_i) + \gamma h_m(x_i))$$

168 • Update the model:

169
$$F_m(x) = F_{m-1}(x) + \gamma_m h_m(x)$$

170 3. Output $F_M(x)$.

171

172 Gradient boosting can be used with decision trees, in particular with CART, of a given
 173 fixed size as weak learners. For this particular situation, Friedman (Friedman, 2002)
 174 proposes a variation of the gradient boosting method that improves each weak learner
 175 quality of fit (Friedman, 2002; Ridgeway, 2007; Hastie et al., 2003; Taieb & Hyndman,
 176 2014; Döpke et al., 2017).

177

178 In the m -th step a generic gradient boosting fits a decision tree $h_m(x)$ to the pseudo-
 179 residuals. If J_m is the number of its leaves, the tree model splits the input space into J_m
 180 separated regions $R_{1m}, \dots, R_{J_m m}$ and obtains a constant value for each region. $h_m(x)$ for
 181 input x is written as the sum (Bühlmann & Hothorn, 2007; Hastie et al., 2003; Taieb &
 182 Hyndman, 2014; Döpke et al., 2017):

$$h_m(x) = \sum_{i=1}^{J_m} b_{jm} I(x \in R_{jm}) \quad (9)$$

183 where b_{jm} is the constant value calculated for the region R_{jm} . These coefficients b_{jm} are
 184 multiplied by some value γ_m , calculated using line search that minimises the loss function,
 185 and then the model is updated:

$$F_m(x) = F_{m-1}(x) + \gamma_m h_m(x); \quad \gamma_m = \arg \min_{\gamma} \sum_{i=1}^n L(y_i, F_{m-1}(x_i) + \gamma h_m(x_i)) \quad (10)$$

186 Friedman (Shapire, 2003; Bühlmann, & Hothorn, 2007) proposed a modification of this
 187 algorithm that chooses a different optimal γ_{jm} for each of the regions, instead of only one
 188 γ_m for the whole tree. This modified algorithm is called TreeBoost. Then, the model is
 189 updated (Bühlmann & Hothorn, 2007; Hastie et al., 2003; Taieb & Hyndman, 2014;
 190 Döpke et al., 2017):

$$F_m(x) = F_{m-1}(x) + \sum_{i=1}^{J_m} \gamma_{jm} I(x \in R_{jm}); \quad \gamma_{jm} = \arg \min_{\gamma} \sum_{x_i \in R_{jm}} L(y_i, F_{m-1}(x_i) + \gamma) \quad (11)$$

191 where the size of trees, J , is the number of terminal nodes in trees and it is a parameter
 192 that can be adjusted for the training data set. It controls the interaction level between
 193 variables in the model. If $J = 2$ (decision stumps), there is no interaction between
 194 variables. With $J = 3$ the model can allow interactions between up to two variables, and
 195 so on. Typically a value between 4 and 8 works well and the results are quite insensitive
 196 to J for these values. $J = 2$ is usually not enough for many applications, and $J > 10$ is often
 197 unnecessary.

198

199 Overfitting the training set can lead to a poor prediction ability. The *regularisation*
 200 techniques are intended to reduce this overfitting effect controlling the training process.

201

202 There are different approaches to attain this aim (Bühlmann and Hothorn 2007; Hastie et
 203 al., 2003; Taieb & Hyndman 2014; Döpke et al., 2017). In particular, the technique used
 204 by the function GBRT is to include in the loss function the so called penalty function
 205 whose aim is to limit the overfitting:

$$L(x) = E(x) + \Omega(x) \quad (12)$$

206 where E can be, for instance, the mean squared error, and Ω is the penalty function that
 207 controls the model complexity, aiding to avoid overfitting by means of increasing the
 208 value of the loss function when the complexity of the model grows, thus penalising it.

209

210 It is also well known that the GBRT technique depends strongly on the following
211 hyperparameters (Chen, & Guestrin, 2016; Chen et al., 2017):

- 212 • *Nrounds*: is the maximum number of iterations performed by the algorithm.
- 213 • η : it controls the learning rate, that is to say, scales the contribution of each tree
214 by a factor η when it is added to the current approximation. Used to prevent
215 overfitting by making the boosting process more conservative. Lower value for η
216 implies larger value for *Nrounds*.
- 217 • γ : It is the minimum loss reduction required to perform another partition on a
218 leaf node of the tree. As it grows, the algorithm is more conservative.
- 219 • Minimum child weight: this parameter avoids the splitting of a node once its
220 sample size has gone under a certain threshold.
- 221 • Maximum Δ step: is a cap value over each tree's weight estimation.
- 222 • Subsample ratio: is the ratio between the training and testing instances.

223 Therefore, it is convenient to use some technique that adjusts these parameters. Usually,
224 the traditional way of performing hyperparameter optimisation has been *grid search*, or
225 a parameter sweep, which is simply an exhaustive searching through a manually specified
226 subset of the hyperparameter space of a learning algorithm. Indeed, the grid search is a
227 brute force method and, as such, almost any optimisation method improves its efficiency.
228 In this study, in order to avoid these problems associated with the grid search method, the
229 differential evolution (DE) metaheuristic technique described below was used (Storn &
230 Price, 1997; Price, Storn, & Lampinen, 2005; Simon, 2013; Yang et al., 2013) with
231 success.

232

233 2.3.2. *The differential evolution (DE) algorithm*

234 In evolutionary computation, differential evolution (DE) is a metaheuristic method that
235 optimises a problem by iteratively trying to improve a candidate solution with regard to
236 a given measure of quality. DE is used for multidimensional real-valued but does not
237 require for the optimisation problem to be differentiable. Therefore, DE can also be used
238 for optimisation problems that are not continuous, are noisy, and change over time, etc.
239 DE optimises a problem by maintaining a population of candidate solutions and creating
240 new candidate solutions by combining existing ones according to its simple formulae, and
241 then keeping whichever candidate solution has the best fitness on the optimisation
242 problem at hand (Storn & Price, 1997).

243

244 The algorithm assumes that the variables of the problem to be optimised are encoded as
245 a vector of real numbers. The length n of these vectors is equal to the number of variables
246 of the problem, and the population is composed of NP vectors (number of parents). A
247 vector \mathbf{x}_p^g is defined, where p is the index of the individual in the population
248 ($p = 1, \dots, NP$) and g is the corresponding generation. Each vector is composed in turn by
249 the variables of the problem $x_{p,m}^g$, where m is the index of the variable in the individual
250 ($m = 1, \dots, n$). It is assumed that the domain of the problem variables is constrained
251 between minimum and maximum values \mathbf{x}_m^{\min} and \mathbf{x}_m^{\max} , respectively. Hence, DE
252 technique is basically composed of four steps:

- 253 • Initialisation;
- 254 • Mutation;
- 255 • Recombination; and
- 256 • Selection.

257 Initialisation is performed at the beginning of the search, and the mutation-recombination-
 258 selection steps are performed repeatedly, until a termination condition or stopping
 259 criterion is satisfied (number of generations, elapsed time, or quality of solution reached,
 260 etc.).

261 *Initialisation*

262 The population is initialised (first generation) randomly, considering the minimum and
 263 maximum values of each variable:

$$\mathbf{x}_{p,m}^1 = \mathbf{x}_m^{\min} + rand(0,1) \cdot (\mathbf{x}_m^{\max} - \mathbf{x}_m^{\min}) \text{ for } p = 1, \dots, NP \text{ and } m = 1, \dots, n \quad (13)$$

264 where $rand(0,1)$ is a random number in the range $[0,1]$.

265 *Mutation*

266 Mutation is the construction of NP noisy random vectors, which are created from three
 267 individuals chosen at random, called target vectors \mathbf{x}_a , \mathbf{x}_b and \mathbf{x}_c . The noisy random
 268 vectors \mathbf{n}_p^t are obtained as follows:

$$\mathbf{n}_p^g = \mathbf{x}_c + F \cdot (\mathbf{x}_a - \mathbf{x}_b) \text{ for } p = 1, \dots, NP \quad (14)$$

269 with p , a , b and c different from each other. F is a parameter that controls the mutation
 270 rate, and is in the range $[0,2]$.

271 *Recombination*

272 After obtaining the NP noisy random vectors, the recombination is performed in a random
 273 manner, comparing them with the original vectors \mathbf{x}_p^g , obtaining the trial vectors \mathbf{t}_m^g as
 274 follows:

$$t_{p,m}^g = \begin{cases} n_{p,m}^g & \text{if } rand(0,1) < GR \\ x_{p,m}^g & \text{otherwise} \end{cases} \text{ for } p = 1, \dots, NP \text{ and } m = 1, \dots, n \quad (15)$$

275 GR is a parameter that controls the recombination rate. Note that the comparison is carried
 276 out variable by variable, so that the test vector will be a mixture of the noisy random
 277 vectors and original vectors.

278 *Selection*

279 Finally, the selection is made simply by comparing the test vectors with the original ones,
 280 so that the vector of the next generation will be the one that has the best value of the
 281 fitness function fit:

$$\mathbf{x}_p^{g+1} = \begin{cases} \mathbf{t}_p^g & \text{if } fit(\mathbf{t}_p^g) > fit(\mathbf{x}_p^g) \\ \mathbf{x}_p^g & \text{otherwise} \end{cases} \quad (16)$$

282 2.4. The goodness-of-fit of this approach

283 The operation physical input variables considered in this research work are shown in
 284 Table 1. Therefore, the total number of predicting variables used to construct the hybrid
 285 DE-GBRT-based model was eight. The output predicted variable is the pressure drop per
 286 unit length ($\Delta p / \Delta L$) and the input variable for filter media type was a category.

287

288 **Table 1** - Set of operation physical input variables used in this study and their names
 289 along with their mean and standard deviation.

290

291 To predict the pressure drop per unit length ($\Delta P / \Delta L$) from other operation parameters,
 292 it is necessary to choose the model that best fits the experimental data. To determine the

293 goodness-of-fit, the two criteria considered here were the coefficient of determination R^2
 294 and the root mean square error (*RMSE*), respectively (Freedman et al., 2007). A dataset
 295 takes values t_i , each of which has an associated modelled value y_i . The former are termed
 296 the observed values and the latter are often referred to as the predicted values. The dataset
 297 variability is measured through different sums of squares as follows (Freedman et al.,
 298 2007):

- 299 • $SS_{tot} = \sum_{i=1}^n (t_i - \bar{t})^2$: the total sum of squares, proportional to the sample variance.
- 300 • $SS_{reg} = \sum_{i=1}^n (y_i - \bar{t})^2$: the regression sum of squares, also termed the explained sum
 301 of squares.
- 302 • $SS_{err} = \sum_{i=1}^n (t_i - y_i)^2$: the residual sum of squares.

303 Note that in the previous sums, \bar{t} is the mean of the n observed data:

$$\bar{t} = \frac{1}{n} \sum_{i=1}^n t_i \quad (17)$$

304 Taking into account the above sums, the coefficient of determination is defined via:

$$R^2 \equiv 1 - \frac{SS_{err}}{SS_{tot}} \quad (18)$$

305 so that a coefficient of determination value of 1.0 points out that the regression curve fits
 306 the data perfectly.

307

308 Similarly, the second ratio used in this research work to measure the goodness-of-fit is
 309 the root mean square error (*RMSE*). It indicates the sample standard deviation of the

310 differences between predicted values and observed values. The *RMSE* is defined for *n*
311 different predictions as follows (Freedman et al., 2007):

$$RMSE \equiv \sqrt{\frac{SS_{err}}{n}} \quad (19)$$

312 2.3.3. *The hybrid DE-GBRT-base model*

313 Additionally, as previously mentioned, the GBRT technique is greatly dependent on the
314 GBRT hyperparameters such as the maximum number of iterations (*Nrounds*), learning
315 rate, minimum loss reduction, minimum child weight, maximum step and subsample
316 ratio. Some methods frequently used to determine suitable hyperparameters are (Hastie,
317 Tibshirani, & Friedman, 2003): grid search, random search, Nelder-Mead search,
318 heuristic search, genetic algorithms, pattern search and so on. Usually, the traditional way
319 of performing hyperparameter optimisation has been *grid search*, or a *parameter sweep*,
320 which selects sets of parameters from a chosen grid and studies the performance of the
321 model for each set. Indeed, the grid search is a brute force method and, as such, almost
322 any optimisation method improves its efficiency. In this study, in order to avoid these
323 problems associated with the grid search method, the differential evolution (DE)
324 metaheuristic technique was used (Price, Storn, & Lampinen, 2005; Simon, 2013; Yang
325 et al., 2013).

326

327 The DE optimisation technique was selected as it appeared to be an appropriate, effective
328 and simple tool for tuning the GBRT parameters. A hybrid model, specifically a novel
329 hybrid DE–GBRT–based model, was constructed taking as its dependent variable the
330 pressure drop per unit length (output variable) from the other eight remaining variables
331 (input variables) found in granular filters (Bové et al., 2015a), studying their effect in

332 order to optimise its calculation through the analysis of the coefficient of determination
333 R^2 with success. Fig. 1 shows the flowchart of this new hybrid DE–GBRT–based model
334 implemented in this research work.

335

336 **Fig. 1** - Flowchart of the new hybrid DE–GBRT–based model.

337

338 Furthermore, cross-validation was the standard technique utilised here for finding the real
339 coefficient of determination (R^2) (Picard & Cook, 1984; Freedman et al., 2007). Indeed,
340 in order to assessment the predictive capacity of the DE–GBRT–based model, a thorough
341 10-fold cross-validation algorithm was implemented in this study (Picard & Cook, 1984).
342 To this end, the regression modelling has been performed with the Extreme Gradient
343 Boosting algorithm, using the *Xgboost library* (Chen, He, Benesty, Khotilovich & Tang,
344 2017) along with the DE technique with the DEoptim package (Ardia, Mullen, Brian, &
345 Peterson, 2016) from the R Project. The initial intervals of the space of solutions used in
346 DE technique are indicated in Table 2.

347

348 It should be noted that sixty population members were used in the DE optimisation. The
349 process stopped if the value of the relative tolerance (10^{-8}) could not be reduced after 30
350 steps or a maximum number of 200 iterations. Under this conditions, the tuning of the
351 parameters required 89 iterations in order to get convergence.

352

353 **Table 2** - Search space for each of the GBRT parameters in the DE tuning process.

354

355 In order to optimise the GBRT parameters, the DE module was used. In this way, the DE
356 looks for the best parameters (maximum number of iterations (rounds), learning rate,
357 minimum loss reduction, minimum child weight, maximum step and subsample ratio) by
358 using the comparison of the cross-validation error in every iteration. The search space is
359 six-dimensional, with one dimension per each parameter. Hence, the objective function
360 or main fitness factor is the coefficient of determination (R^2) in this problem.

361

362 **3. Results and discussion**

363 Table 3 points out the optimal hyperparameters of the best fitted DE–GBRT–based model
364 found with the differential evolution (DE) technique.

365

366 **Table 3** - Optimal hyperparameters of the best fitted GBRT model found with the DE
367 technique.

368

369 Table 4 shows the determination and correlation coefficients for the hybrid DE–GBRT–
370 based model fitted for the pressure drop per unit length in this article.

371

372 **Table 4** - Coefficients of determination (R^2), correlation coefficients (r) and root mean
373 square errors (RMSE) for the hybrid DE–GBRT–based model fitted in this study for the
374 pressure drop per unit length.

375

376 According to these previous statistical calculations, the GBRT technique in combination
377 with the DE optimization is an excellent model for estimating the pressure drop per unit
378 length in granular filters, since the fitted GBRT model with DE has a coefficient of
379 determination R^2 equals 0.77 and a correlation coefficient equals 0.88, respectively.

380

381 These coefficients are similar to those obtained by García-Nieto et al. (2017) using an
382 ABC-MARS model, although the RMSE was slightly smaller with the DE-GBRT model.
383 So, these results show a trustworthy goodness of fit, that is to say, a good agreement is
384 obtained between our model and the observed data.

385

386 An iMac with a processor 3.2 GHz Intel Core i5, with 8GB RAM and Maverick 10.9.5
387 as operating system was used to perform the computation. A time of 773.984 s,
388 approximately 12 min, was necessary for the tuning and construction of the model.

389

390 The importance measure are relative and the addition of all the values for each criteria
391 amounts to one. They are:

- 392 • *Gain*: it is computed taking into account each variable contribution to each tree
393 that appears in the model.
- 394 • *Cover*: it is the relative number of observations of the variable in the model.
- 395 • *Frequency*: it is the relative number of times an independent variable appears in
396 the trees of the obtained model.

397 The most significant measure is *Gain* and thus it has been used to construct the graph of
398 the relative importance of the variables.

399 As an additional result of these calculations, the significance ranking for the three input
400 variables predicting the pressure drop per unit length (output variable) in this complex
401 study is shown in Table 5 and Fig. 2. Therefore, for the DE–GBRT model the most
402 significant variable in pressure drop per unit length prediction is the Flow surface
403 velocity, followed by Average grain size, and finally equivalent diameter.

404

405 **Table 5** - Significance ranking for the variables involved in the best fitted DE–GBRT–
406 based model for the pressure drop per unit length prediction ($\Delta p / \Delta L$) according to
407 criteria *Gain*, *Cover* and *Frequency*.

408

409 **Fig. 2** - Relative importance of the input operation variables to predict the pressure drop
410 per unit length ($\Delta p / \Delta L$) in the fitted DE–GBRT–based model.

411

412 Bearing in mind that the flow surface velocity and average grain size are two variables
413 easy to determine experimentally and the GBRT model indicates that they are the two
414 most important variables, a *simplified* GBRT model was built using only these two
415 variables. The curve predicted with this model is compared with the observed one in Fig.
416 3. The determination coefficient and correlation coefficient for this simplified model were
417 0.78 and 0.88, respectively.

418

419 In conclusion, this work was able to estimate the pressure drop per unit length in
420 agreement with the actual experimental values observed using the DE–GBRT–based
421 model with great accurateness as well as success. Therefore, it was appropriate to use a

422 GBRT model with a DE-based optimisation technique in order to achieve the best
423 effective approach in this regression problem. Because these results agree with the
424 outcome criterion of ‘goodness of fit’ (R^2) the DE-GBRT-based model was an excellent
425 fit to the experimental.

426

427 **Fig. 3** - Comparison between the pressure drop per unit length values observed and
428 predicted, by type of filter, using the DE-GBRT-based simplified model ($R^2 = 0.78$).

429

430 Finally, the residual errors for each observation of the predicted model, calculated as the
431 difference between the predicted and the observed pressure drop per unit length values,
432 by type of filter, using the DE-GBRT-based simplified model, is represented in Fig. 4.

433

434 **Fig. 4** – Residuals for the predicted pressure drop per unit length values, by type of filter,
435 using the DE-GBRT-based simplified model.

436

437 **4. Conclusions**

438 Taking into account the experimental and numerical results, the main findings of this
439 study can be summarised as follows:

- 440 • The new hybrid DE-GBRT-based model used in this work can accurately predict
441 the pressure drop per unit length in different granular media used in sand filters
442 without using as input variable the sphericity, which is a parameter difficult to
443 obtain experimentally.

- 444 • A reasonable coefficient of determination equal to 0.78 was obtained when this
445 hybrid DE–GBRT–based model was applied to the experimental pressure drop
446 dataset.
- 447 • The significance order of the input variables involved in the prediction of the
448 pressure drop per unit length in granular filters was set. This is one of the main
449 findings in this work. Specifically, input variable Flow surface velocity could be
450 considered the most influential parameter in the prediction of the pressure drop
451 per unit length. In this regard, it is also important to highlight the influential role
452 of the Average grain size in the dependent variable pressure drop per unit length.
- 453 • Taking into account the results of the previous point, and for practical reasons, as
454 the two most important variables are relatively easy to obtain, a simplified GBRT
455 model that used only these variables was developed with a comparatively very
456 good coefficient of determination.
- 457 • The influence of the hyperparameters involved in the GBRT approach to predict
458 pressure drop per unit length regression performance was established.
- 459 • The results verified that the hybrid DE–GBRT–based regression method
460 significantly improved the generalisation capability achievable with only the
461 GBRT–based regressor. Thus, input data from other filtered materials used in
462 microirrigation can be processed to predict the pressure drop measuring only a
463 few key variables.

464 In summary, this innovative methodology presented could be applied to other filtration
465 processes with similar or distinct filter media types with success, but it is always
466 necessary to take into account the characteristics of each filter and experiment.
467 Consequently, an effective DE–GBRT–based model is a good practical solution to the

468 problem of predicting the pressure drop in sand media filters that are used in
469 microirrigation systems.

470

471 **Acknowledgements**

472 Authors wish to acknowledge the computational support provided by the Department of
473 Mathematics at University of Oviedo as well as financial support of the Spanish Ministry
474 of Economy and Competitiveness through Grant AGL2015-63750-R. Additionally, we
475 would like to thank Anthony Ashworth for his revision of English grammar and spelling
476 of the manuscript.

477

478 **References**

- 479 Arbat, G., Pujol, T., Puig-Bargués, J., Duran-Ros, M., Montoro, L., & Barragán, J. (2013).
480 An experimental and analytical study to analyze hydraulic behaviour of nozzle-type
481 underdrains in porous media filters. *Agricultural Water Management*, 126, 64–74.
- 482 Ardia, D., Mullen, K. M., Peterson, B. G., & Ulrich, J. (2016). DEoptim: Differential
483 evolution in R. version 2.2-4.
- 484 Barreiros, F. M., Ferreira, P. J., & Figueirido, M. M. (1996). Calculating shape factors
485 from particle sizing data. *Particle & Particle Systems Characterization*, 13(6), 368–
486 373.
- 487 Bové, J., Arbat, G., Duran-Ros, M., Pujol, T., Velayos, J., Ramírez de Cartagena, F., &
488 Puig-Bargués, J. (2015a). Pressure drop across sand and recycled glass media used in
489 micro irrigation filters. *Biosystems Engineering*, 137, 55–63.

490 Bové, J., Arbat, G., Pujol, T., Duran-Ros, M., Ramírez de Cartagena, F., Velayos, J., &
491 Puig-Bargués, J. (2015b). Reducing energy requirements for sand filtration in
492 microirrigation: improving the underdrain and packing. *Biosystems Engineering*, 140,
493 67–78.

494 Breiman, L., Friedman, J.H., Olshen, R.A., & Ston, C.J. (1984). *Classification and*
495 *regression trees*. Monterey, CA, USA: Wadsworth and Brooks/Cole.

496 Bühlmann, P., & Hothorn, T. (2007). Boosting algorithms: regularization, prediction and
497 model fitting. *Statistical Science*, 22(4), 477–505.

498 Burt, C.M. (2010). Hydraulics of commercial sand media filter tanks used for agricultural
499 drip irrigation. ITRC Report No. R 10001. San Luis Obispo, California: Irrigation
500 Training and Research Center.

501 Chen, T., & Guestrin, C. (2016). XGBoost: a scalable tree boosting system. In
502 Proceedings of the 22nd ACM SIGKDD International Conference on Knowledge
503 Discovery and Data Mining (pp. 785–794). San Francisco, California, USA: ACM
504 Publishers.

505 Chen, T., He, T., Benesty, M., Khotilovich, V., & Tang, Y. (2017). xgboost: Extreme
506 gradient boosting. R package version 0.6-4. [https://CRAN.R-](https://CRAN.R-project.org/package=xgboost)
507 [project.org/package=xgboost](https://CRAN.R-project.org/package=xgboost).

508 Clark, G. A., Haman, D. Z., Prochaska, J. F. & Yitayew, M. (2007). General system
509 design principles. In F.R.Lamm, F.R., J.E.Ayars, & F.S.Nakayama. (Eds.),
510 Microirrigation for Crop Production (pp.161–220). Amsterdam: Elsevier.

511 Clerc, M. (2006). *Particle swarm optimization*. London, UK: Wiley-ISTE.

512 Döpke, J., Fritsche, U., Pierdzioch, C. (2017). Predicting recessions with boosted
513 regression trees. *International Journal of Forecasting*, 33, 745–759.

514 Dorigo, M., & Stützle, T. (2004). *Ant colony optimization*. Cambridge, Massachusetts,
515 USA: Bradford Publisher, The MIT Press.

516 Droste, R. L. (1997). *Theory and practice for water and wastewater treatment*. New
517 York: John Wiley & Sons.

518 Duran-Ros, M., Puig-Bargués, J., Arbat, G., Barragán, J. & Ramírez de Cartagena, F.
519 (2009). Performance and backwashing efficiency of disc and screen filters in
520 microirrigation systems. *Biosystems Engineering*, 103(1), 35–42.

521 Eberhart, R. C., Shi, Y., & Kennedy, J. (2001). *Swarm intelligence*. San Francisco:
522 Morgan Kaufmann.

523 Elbana, M., Ramírez de Cartagena, F., & Puig-Bargués, J. (2013). New mathematical
524 model for computing head loss across sand media filter for microirrigation systems.
525 *Irrigation Science*, 31(3), 343–349.

526 Feoktistov, V. (2006). *Differential evolution: in search of solutions*. New York: Springer.

527 Freedman, D., Pisani, R., & Purves, R. (2007). *Statistics*. New York: W.W. Norton &
528 Company.

529 Friedman, J. H., Hastie, T., & Tibshirani, R. (2000). Additive logistic regression: A
530 statistical view of boosting. *Annals of Statistics*, 28(2), 337–407.

531 Friedman, J. H. (2001). Greedy function approximation: A gradient boosting machine.
532 *Annals of Statistics*, 29(5), 1189–1232.

533 Friedman, J. H. (2002). Stochastic gradient boosting. *Computational Statistics & Data*
534 *Analysis*, 38(4), 367–378.

- 535 García-Nieto, P.J., García-Gonzalo, E., Bové, J., Arbat, G., BovéM. & Puig-Bargués, J.
536 (2017). Modeling pressure drop produced by different filtering media in
537 microirrigation sand filters using the hybrid ABC-MARS-based approach, MLP
538 neural network and M5 model tree. *Computers and Electronics in Agriculture*, 139,
539 65–74.
- 540 Hastie, T., Tibshirani, R., & Friedman, J. H. (2003). *The elements of statistical learning*.
541 New York: Springer-Verlag.
- 542 Horan, N., & Lowe, M. (2007). Full-scale trials of recycled glass as tertiary filter medium
543 for wastewater treatment. *Water Resources*, 41(1), 253–259.
- 544 Johnson, N. E., Ianiuk, O., Cazap, D., Liu, L., Starobin, D., Dobler, G., & Ghandehari,
545 M. (2017). Patterns of waste generation: A gradient boosting model for short-term
546 waste prediction in New York City. *Waste Management*, 62, 3–11.
- 547 Lamm, F.R. & Rogers, D.H. (2017). Longevity and performance of a subsurface drip
548 irrigation system. *Transactions of the ASABE*, 60(3), 931–939.
- 549 Landry, M., Erlinger, T. P., Patschke, D., & Varrichio, C. (2016). Probabilistic gradient
550 boosting machines for GEFCom2014 wind forecasting. *International Journal of*
551 *Forecasting*, 32(3), 1061–1066.
- 552 Mayr, A., Binder, H., Gefeller, O., & Schmid, M. (2014a). The evolution of boosting
553 algorithms: From machine learning to statistical modelling. *Methods of Information*
554 *in Medicine*, 6(1), 419–427.
- 555 Mayr, A., Binder, H., Gefeller, O., & Schmid, M. (2014b). Extending statistical boosting:
556 An overview of recent methodological developments. *Methods of Information in*
557 *Medicine*, 6(2), 428–435.

- 558 Mesquita, M., Testezlaf, R., & Ramirez, J.C.S. (2012). The effect of media bed
559 characteristics and internal auxiliary elements on sand filter head loss. *Agricultural*
560 *Water Management*, 115, 178–185.
- 561 Natekin, A., & Knoll, A. (2013). Gradient boosting machines, a tutorial. *Frontiers in*
562 *Neurorobotics*, 7, 1–21
- 563 Nielsen, D. (2016). Tree Boosting with XGBoost. Master of Science in Physics and
564 Mathematics. Norwegian University of Science and Technology.
- 565 Olsson, A. E. (2011). Particle swarm optimization: theory, techniques and applications.
566 New York: Nova Science Publishers.
- 567 Persson, C., Bacher, P., Shiga, T., & Madsen, H. (2017). Multi-site solar power
568 forecasting using gradient boosted regression trees. *Solar Energy*, 150, 423–436.
- 569 Picard, R., & Cook, D. (1984). Cross-validation of regression models. *Journal of the*
570 *American Statistical Association*, 79(387), 575–583.
- 571 Price, K., Storn, R.M., & Lampinen, J.A. (2005). *Differential evolution: a practical*
572 *approach to global optimization*. Berlin: Springer.
- 573 Ridgeway, G. (2007). Generalized boosted models: a guide to the GBM package.
574 <http://www.saedsayad.com/docs/gbm2.pdf>. Accessed 3 August 2007
- 575 Ridgeway, G. (2017). gbm: Generalized boosted regression models. R package version
576 2.1.1. <http://CRAN.R-project.org/package=gbm>. Accessed 21 March 2017
- 577 Rocca, P., Oliveri, G., & Massa, A. (2011). Differential evolution as applied to
578 electromagnetics. *IEEE Antennas and Propagation Magazine*, 53 (1), 38–49.
- 579 Simon, D. (2013). *Evolutionary optimization algorithms*. New York: Wiley.

580 Schapire, R. E. (2003). The boosting approach to machine learning an overview. In D. D.
581 Denison, M. H. Hansen, C. C. Holmes, B. Mallick, & B. Yu (Eds.), *Nonlinear*
582 *estimation and classification* (vol. 171, pp. 149–171), Lecture notes in statistics.
583 Berlin: Springer.

584 Storn, R., & Price, K. (1997). Differential evolution - a simple and efficient heuristic for
585 global optimization over continuous spaces. *Journal of Global Optimization*, 11, 341–
586 359.

587 Taieb, S. B., & Hyndman, R. J. (2014). A gradient boosting approach to the kaggle load
588 forecasting competition. *International Journal of Forecasting*, 30(2), 382–394.

589 Vapnik, V. (1998). *Statistical learning theory*. New York: Wiley-Interscience.

590 Wu, W., Chen, W., Liu, H., Yin, S., Bao, Z., Niu, Y. (2014a). A dimensional analysis
591 model for the calculation of head loss due to disc filters in drip irrigation systems.
592 *Irrigation and Drainage*, 63(3), 349–358.

593 Wu, W., Chen, W., Liu, H., Yin, S., Niu, Y. (2014b). A new model for head loss
594 assessment of screen filters developed with dimensional analysis in drip irrigation
595 systems. *Irrigation and Drainage*, 63(4), 523–531.

596 Yang, X.–S., Cui, Z., Xiao, R., Gandomi, A.H., & Karamanoglu, M. (2013). *Swarm*
597 *intelligence and bio-inspired computation: theory and applications*. London:
598 Elsevier.

599 Yurdem, H., Demir, V., & Degirmencioglu, A. (2008). Development of a mathematical
600 model to predict head losses from disc filters in drip irrigation systems using
601 dimensional analysis. *Biosystems Engineering*, 100(1), 14–23.

602 Yurdem, H., Demir, V., & Degirmencioglu, A. (2010). Development of a mathematical
603 model to predict clean water head losses in hydrocyclone filters in drip irrigation
604 systems using dimensional analysis. *Biosystems Engineering*, 105(4), 495–506.

605 Zhong, Q., Zheng, T.; Liu, H., & Li, C. (2015). Development of head loss equations for
606 self-cleaning screen filters in drip irrigation systems using dimensional analysis.
607 *Biosystems Engineering*, 133, 116–127.

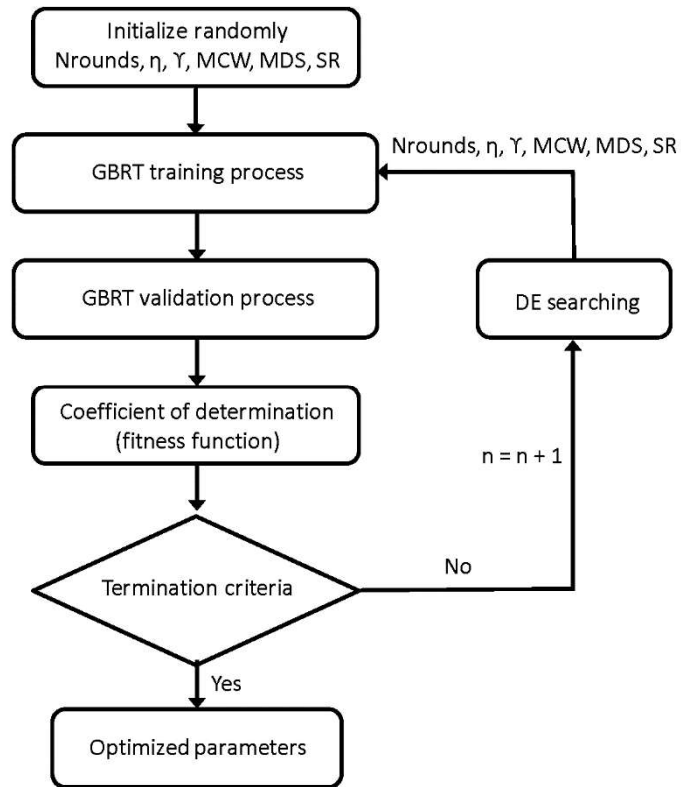


Fig. 1 - Flowchart of the new hybrid DE–GBRT–based model.

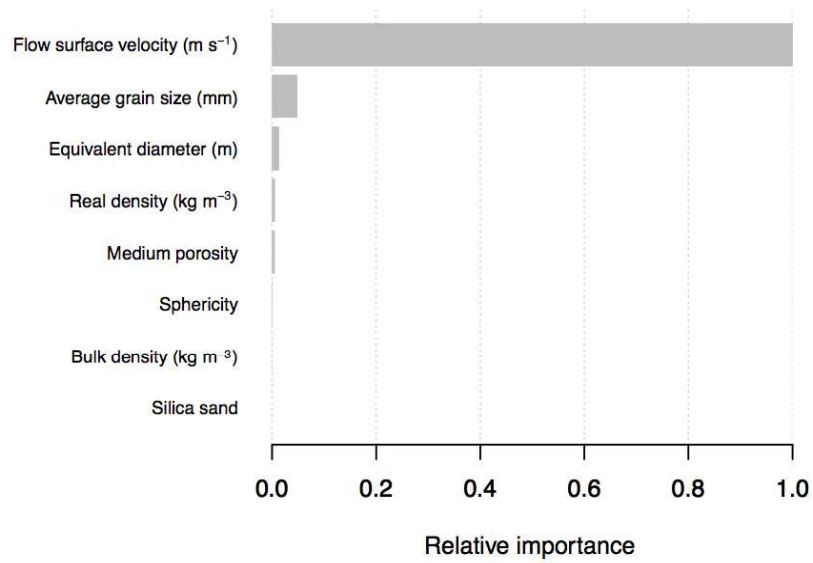


Fig. 2 - Relative importance of the input operation variables to predict the pressure drop per unit length ($\Delta p / \Delta L$) in the fitted DE-GBRT-based model.

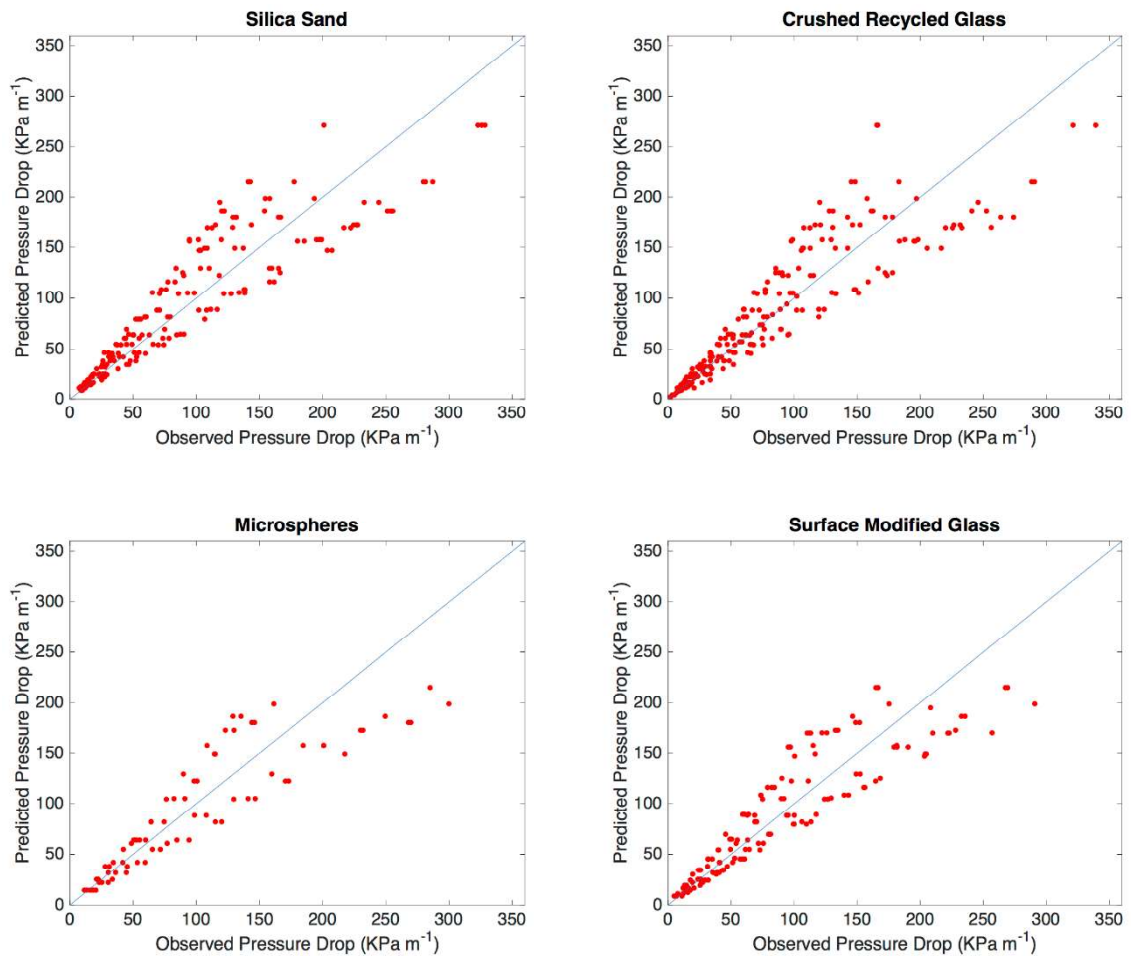


Fig. 3 - Comparison between the pressure drop per unit length values observed and predicted, by type of filter, using the DE-GBRT-based simplified model ($R^2 = 0.78$).

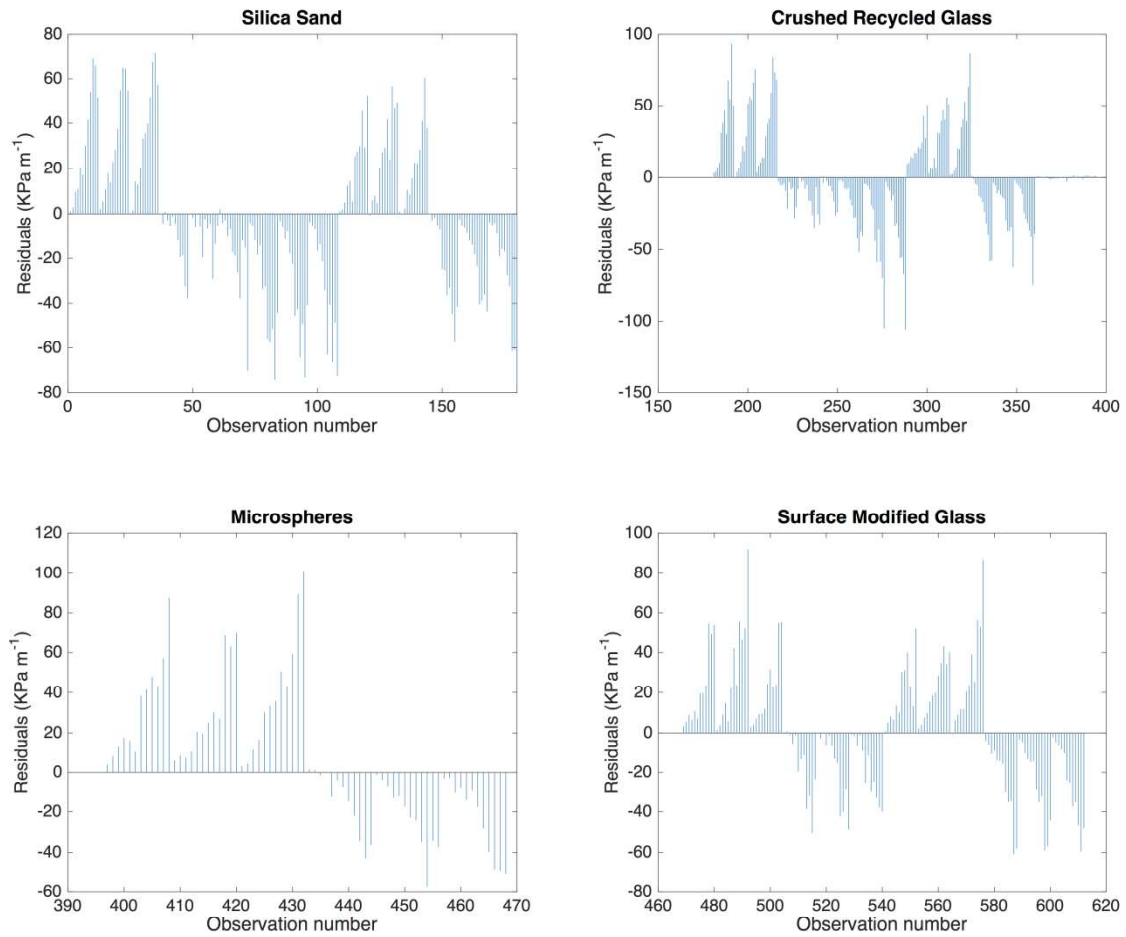


Fig. 4 – Residuals for the predicted pressure drop per unit length values, by type of filter, using the DE-GBRT-based simplified model.

Table 1 - Set of operation physical input variables used in this study and their names along with their mean and standard deviation.

Input variables	Name of the variable	Mean	Standard deviation
Filter media type	Filter_type	--	--
Bulk density (kg m ⁻³)	Density_b	1397	88.77
Real density (kg m ⁻³)	Density_r	2471	62.58
Medium porosity	Porosity	0.4324	0.03119
Equivalent diameter (m)	Diameter	0.7935	0.1761
Sphericity	Sphere	0.7637	0.1314
Flow surface velocity (m s ⁻¹)	Velocity	0.01421	0.006594
Average grain size (mm)	Grain_size	0.7576	0.1176

Table 2 - Search space for each of the GBRT parameters in the DE tuning process.

GBRT hyperparameters	Lower limit	Upper limit
Rounds	1	100
η	0.1	1
γ	0	30
Minimum child weight (MCW)	1	30
Maximum Δ step (MDS)	0	30
Subsample ratio	0.5	1

Table 3 - Optimal hyperparameters of the best fitted GBRT model found with the DE technique.

GBRT hyperparameters	Optimal values
Rounds	60
η	0.51
γ	0.17
Minimum child weight (<i>MCW</i>)	4.7
Maximum Δ step (<i>MDS</i>)	15
Subsample ratio (<i>SR</i>)	0.87

Table 4 - Coefficients of determination (R^2), correlation coefficients (r) and root mean square errors (RMSE) for the hybrid DE–GBRT–based model fitted in this study for the pressure drop per unit length.

Model	Coef. of determination (R^2)/correlation coef. (r)	RMSE
DE–GBRT	0.7741/0.8798	30.15

Table 5 - Significance ranking for the variables involved in the best fitted DE-GBRT-based model for the pressure drop per unit length prediction ($\Delta p / \Delta L$) according to criteria Gain, Cover and Frequency.

Input variable	<i>Gain</i>	<i>Cover</i>	<i>Frequency</i>
Flow surface velocity	9.32×10^{-1}	0.7025	0.5593
Average grain size	4.50×10^{-2}	0.0606	0.1282
Equivalent diameter	1.22×10^{-2}	0.0643	0.0459
Real density	4.96×10^{-3}	0.0658	0.0763
Medium porosity	4.66×10^{-3}	0.0603	0.1467
Sphericity	5.79×10^{-4}	0.0266	0.0280
Bulk density	1.41×10^{-4}	0.0176	0.0137
Silica sand	3.11×10^{-6}	0.0021	0.0017